Differential Impact of Fluid Shear Stress and YAP/TAZ on BMP/TGF-β Induced Osteogenic Target Genes

Maria Reichenbach, Paul-Lennard Mendez, Carolina da Silva Madaleno, Vladimir Ugorets, Paul Rikeit, Stefan Boerno, Jerome Jatzlau, and Petra Knaus*

Bone is a remarkable dynamic structure, which integrates mechanical and biochemical signaling inputs. Interstitial fluid in the intramedullary space transmits signals derived from compression-induced fluid shear stress (FSS) to stimulate osteoblasts for bone formation. Using a flow system and human osteoblasts, this study demonstrates how BMP/TGF-β signaling integrates stimuli derived from FSS and YAP/TAZ and confirms these findings by transcriptome analyses. Here, FSS positively affects the phosphorylation of both SMAD1/5 and SMAD2/3, the respective BMP- and TGFβ-R-SMADs. Increase in phosphorylated SMAD1/5 levels affects distinct target genes, which are susceptible to low levels of phosphorylated SMADs (such as ID1–3) or dependent on high levels of phosphorylated SMAD1/5 (NOG, noggin). Thus, FSS lowers the threshold for genes dependent on high levels of phosphorylated SMAD1/5 when less BMP is available. While the impact of FSS on direct BMP target genes is independent of YAP/TAZ, FSS acts cooperatively with YAP/TAZ on TGF-β target genes, which are shared by both pathways (such as CTGF). As mechanical stimuli are key in bone regeneration, their crosstalk to biochemical signaling pathways such as BMP and TGF-β and YAP/TAZ acts on different levels, which allows now to think about new and more specified intervention strategies for age-related bone loss.

1. Introduction

Bone is a remarkable tissue as it matches mechanical demands and functions with a matrix of unique biophysical and biochemical properties.[1,2] The structure and architecture of bone is susceptible to conditions such as aging, pathologies as osteoporosis, but also to physical exercise and nutrition supply.[3,4] Its matrix is constantly remodeled to adapt to its changing mechanical microenvironment and to maintain skeletal functions.[5] Cells within bone, therefore, sense mechanical inputs to translate them into biological responses. Pressure gradients, e.g., from mechanical loading and locomotion, induce flow of the interstitial fluid in the intramedullary space of the bone, thereby stimulating osteoblasts.[6,7] Jacobs et al.[8] have shown that immortalized human fetal osteoblasts (hFOBs) respond to steady and pulsatile unidirectional shear stress but not to oscillatory shear stress, indicating an involvement of chemotransport facilitated by unidirectional shear stress. Osteoblasts are derived from mesenchymal stem cells (MSCs) via osteogenic differentiation, a process itself tightly regulated by both mechanical forces and biochemical factors, which collectively shape processes such as bone development, homeostasis, and repair.[9]

One of the major instructive factors for bone formation (osteogenesis) is bone morphogenetic proteins (BMPs), secreted growth factors belonging to the transforming growth factor-β (TGFβ) superfamily. BMPs signal via binding to heterotetrameric receptor complexes consisting of two type I and type II serine/threonine kinase receptors (BMPR1 and BMPR2), initiating intracellular SMAD and non-SMAD responses. Activated BMP type I receptors phosphorylate SMAD1/5/8, allowing their heterotrimeric complex formation with SMAD4 and subsequent translocation into the nucleus to regulate transcription of target genes, including family members of inhibitor of differentiation (ID) genes.[10,11] BMPs are therefore important players of osteogenic differentiation, and mutations in BMP pathway components can result in severe bone pathologies such as fibrodysplasia ossificans progressiva (FOP) or osteoporosis.[12,13] Recombinant human BMP-2 and BMP-7 are in clinical use to support fracture healing,[14,15] nonetheless their physiological concentration is several magnitudes lower then applied treatment

Dr. M. Reichenbach, P.-L. Mendez, C. da Silva Madaleno, V. Ugorets, Dr. P. Rikeit, Dr. J. Jatzlau, Prof. P. Knaus
Institute of Chemistry/Biochemistry
Freie Universität Berlin
Thielallee 63, Berlin 14195, Germany
E-mail: petra.knaus@fu-berlin.de

C. da Silva Madaleno, Dr. P. Rikeit, Dr. J. Jatzlau
Berlin-Brandenburg School for Regenerative Therapies (BSRT)
Charité—Universitätsmedizin Berlin
Föhrer Str. 15, Berlin 13353, Germany

P.-L. Mendez
International Max Planck Research School for Biology and Computation
Max Planck Institute for Molecular Genetics
Ihnestr. 63, Berlin 14195, Germany

Dr. S. Boerno
Sequencing Core Facility
Max Planck Institute for Molecular Genetics
Ihnestr. 63, Berlin 14195, Germany

doses,[16,17] and side effects from excess concentrations of these growth factors have been reported.[18] Current research strategies focus on regulatory mechanisms and crosstalks to other pathways to collectively enhance cellular responses to physiological BMP concentrations and to improve the efficacy of regenerative therapies for bone diseases. Of particular interest is the crosstalk with mechanosensitive signaling pathways, as it was shown that mechanical stimuli integrate into the BMP signaling cascade.[19–21] In an in vivo rat osteotomy model, mechanical loading enhanced the efficacy of BMP-2 application on fracture healing.[22] Likewise, Kopf et al. used a 3D bioreactor system to show that BMP-2 stimulation and concurrent mechanical loading lead to increased intensity and duration of SMAD1/5/8 phosphorylation, as well as increased ID transcription in hFOBs.[19]

Actin fibers transmit, generate, and are subjected to mechanical forces and have been shown to act as tension sensors, modulating their affinity for binding partners depending on the filament stress load.[23,24] Furthermore, recent work has shown that an intact actin cytoskeleton is crucial for osteogenic differentiation of MSCs.[25,26] Many actin binding proteins were identified as crucial components in signal transduction pathways such as the Hippo cascade.[27–29] The Hippo pathway with its nuclear effectors Yes-associated protein (YAP, gene name YAP1) and transcriptional coactivator with PDZ-binding motif (TAZ, gene name WWTR1) has recently been appreciated as a major mechanosensitive signaling cascade,[30] Originally found to be regulated by cell density,[31] it was later discovered that cell geometry and cell spreading, substrate stiffness and rigidity,[32] fluid flow,[33] and cytoskeletal tension[27] govern Hippo-YAP/TAZ activity. Generally, in cells that are spread over a large area, grow on stiff substrates, or generate intracellular tension, YAP/TAZ translocate in the nucleus, where they act as transcriptional coactivators or corepressors together with other transcription factors, guiding the expression of genes involved in cell cycle control, apoptosis, differentiation, and migration.[34–38] YAP/TAZ activity is canonically regulated by LATS protein kinase, which is activated by phosphorylation in response to various inputs.[31] Activated LATS phosphorylates YAP/TAZ, which leads to their retention in the cytoplasm and therefore inactivation.[39] Interestingly, actin stress fibers impact Hippo signaling at the level of LATS or upstream, as disruption of F-actin leads to activation of LATS and therefore inactivation of YAP/TAZ.[40] The majority of YAP/TAZ effects are mediated via interaction with TEAD family transcription factors;[41] however, other partners such as p73,[42] KLF5,[43] ERBB4,[44] or RUNX2[45] have also been identified. Of note, YAP and TAZ also influence SMAD-mediated transcriptional activity.[46–49] By direct binding of YAP to SMADs, BMP-induced SMAD transcriptional activity is enhanced as it was shown during neuronal differentiation of mouse embryonic stem cells (mESCs).[46] YAP/TAZ also interact with TGF-β regulated SMAD2/3 in a cell-density-dependent manner, dictating their subcellular localization.[48,49] YAP/TAZ regulate expression of extracellular matrix proteins (e.g., COL1A1), and thereby play an important role in tissue regeneration and remodeling.[50–52] In bone, extracellular matrix proteins provide a scaffold for the deposition of calcified minerals, thereby generating macroscale mechanical

stability and flexibility.[53,54] The major scaffold here is collagen type I (COL1A1 and COL1A2), whereas osteopontin (SPP1) and osteocalcin (OCN) contribute to the nanoscale mechanical behavior.[53,55–57] Matrix metalloproteases like MMP2 and MT1-MMP degrade extracellular matrix (ECM) to direct MSC—osteoblast commitment and differentiation via activation of YAP/TAZ.[58] Thus, this complex ECM network itself instructs osteogenesis.

In this study, we demonstrate that osteogenic differentiation of human osteoblasts is promoted by mechanical inputs elicited by fluid shear stress (FSS) and mediated via YAP/TAZ and the expression of ECM genes. To understand the underlying mechanism, we analyzed the impact of YAP/TAZ on SMAD-induced BMP/TGF-β signaling in proliferative and differentiating bone precursor cells. Here, we used hFOBs as a model cell line, as they were shown to integrate mechanical stimuli into the BMP signaling cascade and respond similar as MSCs.[19,59,60] We performed a comparative whole-genome expression profiling using RNA sequencing (RNA-Seq) of hFOBs, depleted for YAP/TAZ and stimulated with BMP-2. Based on these data, we propose that YAP/TAZ influences both SMAD1/5 and SMAD2/3 phosphorylation and subsequent BMP/TGF-β-SMAD-dependent gene transcription through different mechanisms including SMAD degradation, dephosphorylation, and distinct transcriptional complex formation.

2. Results

2.1. FSS Promotes Osteogenic Differentiation with Differential YAP/TAZ Impact

The osteoblastic niche harbors osteoblasts in the bone marrow, which line the endosteal bone. Mechanical inputs result in FSS in the intramedullary space inducing mechanotransduction pathways (**Figure 1**a).[61] To test whether FSS impinges on osteogenic differentiation via actin remodeling and subsequent YAP/TAZ activation, we first subjected hFOBs to 5 dyn cm^{-2} FSS in vitro for 1 h and analyzed their actin cytoskeleton organization (Figure 1b). We show that FSS increased perinuclear actin fiber intensity already after 1 h (Figure 1b). Further, FSS promoted LATS1 phosphorylation (Figure 1c) thereby indicating inhibition of YAP/TAZ's transcriptional activity. This was confirmed by analyzing the expression of CYR61, a YAP/TAZ target gene (Figure 1d). Next, we induced osteogenic differentiation of hFOB cells via a temperature shift from 33.5 to 39.5 °C.[62] Actin fibers rearranged and aligned 3 days after induction of osteogenesis, which was quantified by measuring their orientation towards a given axis using fast Fourier transformation (FFT) (**Figure 2**a).[63] Interestingly, under those osteogenic differentiation conditions, FSS increased CYR61 gene expression, indicating an increase in YAP/TAZ activity (Figure 2b). Furthermore, simultaneous differentiation and FSS stimulation enhanced expression of osteogenic matrix genes COL1A1 and SPP1, whereas FSS had no impact on ALP (Figure 2c). ALP was only induced by differentiation conditions and not further supported by FSS. This suggests that FSS promotes osteogenic differentiation through the regulation of FSS-sensitive genes, such as COL1A1 and SPP1, highlighting the importance of
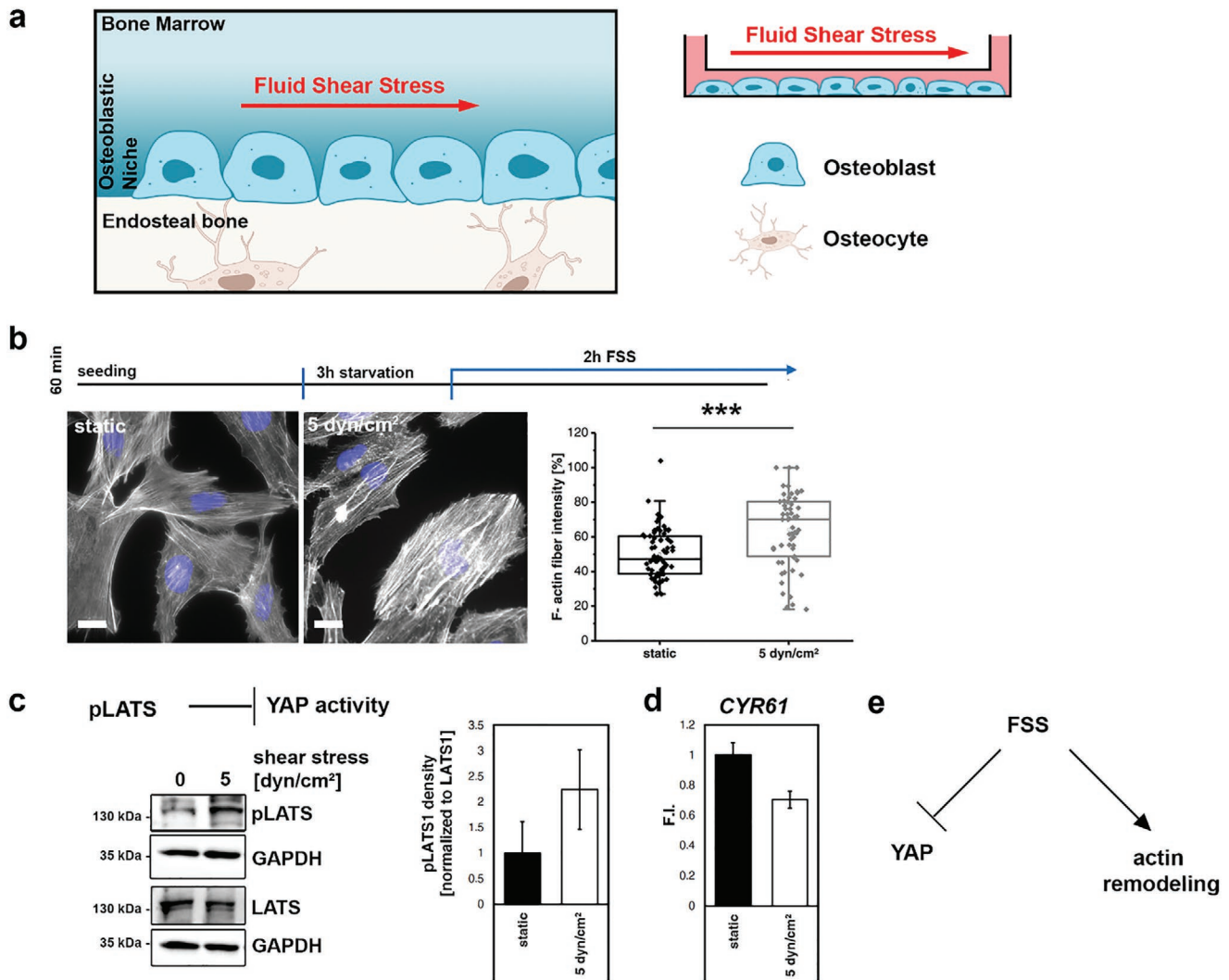
Figure 1. FSS enhances stress fiber formation and induces LATS phosphorylation resulting in decreased YAP-dependent target gene expression. a) Mechanical loading of the bone results in unidirectional FSS in the bone marrow exciting osteoblasts, which line the endosteal bone. Schematic drawing of the flow chamber cultivated with cells, which is used to apply FSS on an hFOB cell line. b) Actin fibers were stained using phalloidin and nuclei were stained using DAPI (blue). Scale bars = 20 µm. c) Representative western blot analysis and densitometric analysis of three independent experiments of pLATS in hFOBs pretreated with 5 dyn cm^{-2} FSS for 4 h. d) qPCR analysis of YAP target gene expression CYR61 in hFOBs pretreated with 5 dyn cm^{-2} FSS for 1 h. e) Graphical illustration depicting the impact of 1 h FSS on YAP activity and actin cytoskeleton.

mechanically induced matrix deposition in osteogenic differentiation. Taken together, we show that FSS promotes actin remodeling and osteogenic differentiation of osteoblasts, while the cotranscriptional support by YAP/TAZ is dynamic and reduced under short term but increased upon long-term FSS stimulation.

2.2. FSS and YAP Regulate Genes Involved in Bone-Specific ECM Organization

Osteogenesis is influenced by a variety of factors including growth factors of the TGF-β superfamily and by mechanical stimuli. Consequently, we hypothesize that the YAP/TAZ pathway is intertwining with TGF-β and BMP signaling resulting in osteogenic differentiation. Thus, we performed

a comprehensive RNA-Seq study including both YAP/TAZ depletion by siRNA and BMP stimulation conditions. Here, we determined 1381 differentially expressed genes, from which 1331 genes (red frame) (**Figure 3**a) are exclusively regulated by YAP/TAZ, 15 genes exclusively after 1 h BMP-2 stimulation, and 35 genes in both conditions (Venn diagram, Figure 3a). The 1331 genes exclusively regulated upon YAP/TAZ depletion were subjected to hierarchical cluster analysis. The majority of genes (cluster A; 911 genes) are upregulated in the absence of YAP/TAZ, indicating that they are repressed by YAP/TAZ. Among those are for example, genes encoding ECM and ECM remodeling proteins, such as SPP1, COL3A1, MMP14, and MMP16. In contrast, 420 genes (cluster B) are positively regulated by YAP/TAZ, including CYR61, CTGF, and ALP. Further, genes associated with "osteoblast differentiation" were found deregulated in the absence of YAP/TAZ, highlighting an involvement of

**ADVANCED
SCIENCE NEWS**

www.advancedsciencenews.com

**ADVANCED
BIOLOGY**

www.advanced-bio.com
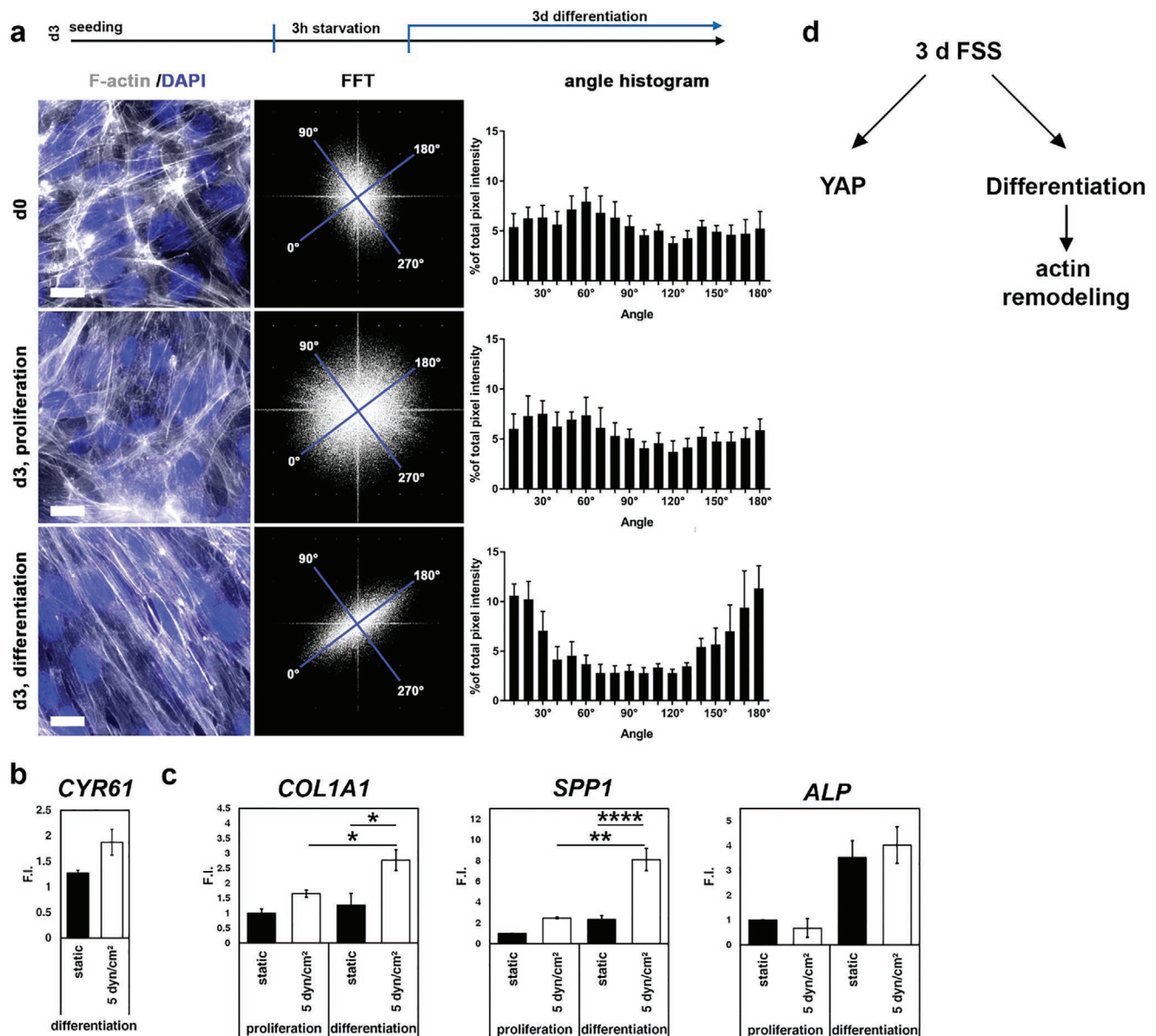
Figure 2. FSS promotes osteogenic differentiation and YAP/TAZ target gene expression, whereby the actin cytoskeleton reorients during osteogenic differentiation. a,b) Densely plated hFOBs were starved in medium containing 2% FCS for 3 h (d0) and then cultured at proliferating (d3, 34 °C) or at differentiating (d3, 39.5 °C) conditions for 72 h under static conditions or 5 dyn cm^{-2} FSS as indicated. a) Cells were fixed and stained for actin cytoskeleton using phalloidin and nuclei using DAPI. Angle orientation was quantified using fast Fourier transformation (FFT) to depict alignment of the actin cytoskeleton. b) qPCR analysis of CYR61 mRNA. c) qPCR analysis of COL1A1, SPP1, and ALP mRNA. Data are presented as mean ± SEM of three independent experiments, two-way ANOVA with Bonferroni post hoc test, compared to corresponding static control samples. d) Schematic drawing illustrating the influence of 3D FSS on YAP and osteogenic differentiation.

YAP/TAZ in this biological process (Figure 3b). Further, functional enrichment of biological processes using DAVID Bioinformatics Resources 6.8[64] identified "ECM organization" and "TGF-β/BMP signaling" as overrepresented biological processes regulated by YAP/TAZ. In detail, genes encoding for integrins, collagens, and laminins that belong to the biological process "ECM organization" were mainly upregulated upon YAP/TAZ depletion (Figure 3b, cluster A). Moreover, we found that the BMP/TGF-β signaling pathway genes (Figure 3b) encode ligands and ligand-binding proteins such as GDF5, GDF15,

TGFB2, TGFB3, LTBP1, and LTBP3, the BMP coreceptor RGMB and BMP inhibitor BMPER, indicating a crosstalk of YAP/TAZ with the BMP/TGF-β pathway on multiple levels.

Therefore, we next asked how BMP2 stimulation intertwines with the FSS- and/or YAP-dependent target gene regulation. For instance, CYR61, SPP1, and COL1A1 are all relevant for osteogenic differentiation but members of different gene clusters and regulated individually by these stimuli. While all three are upregulated by FSS, the impact of BMP2 and/or YAP on these genes is different and might explain their individual functional
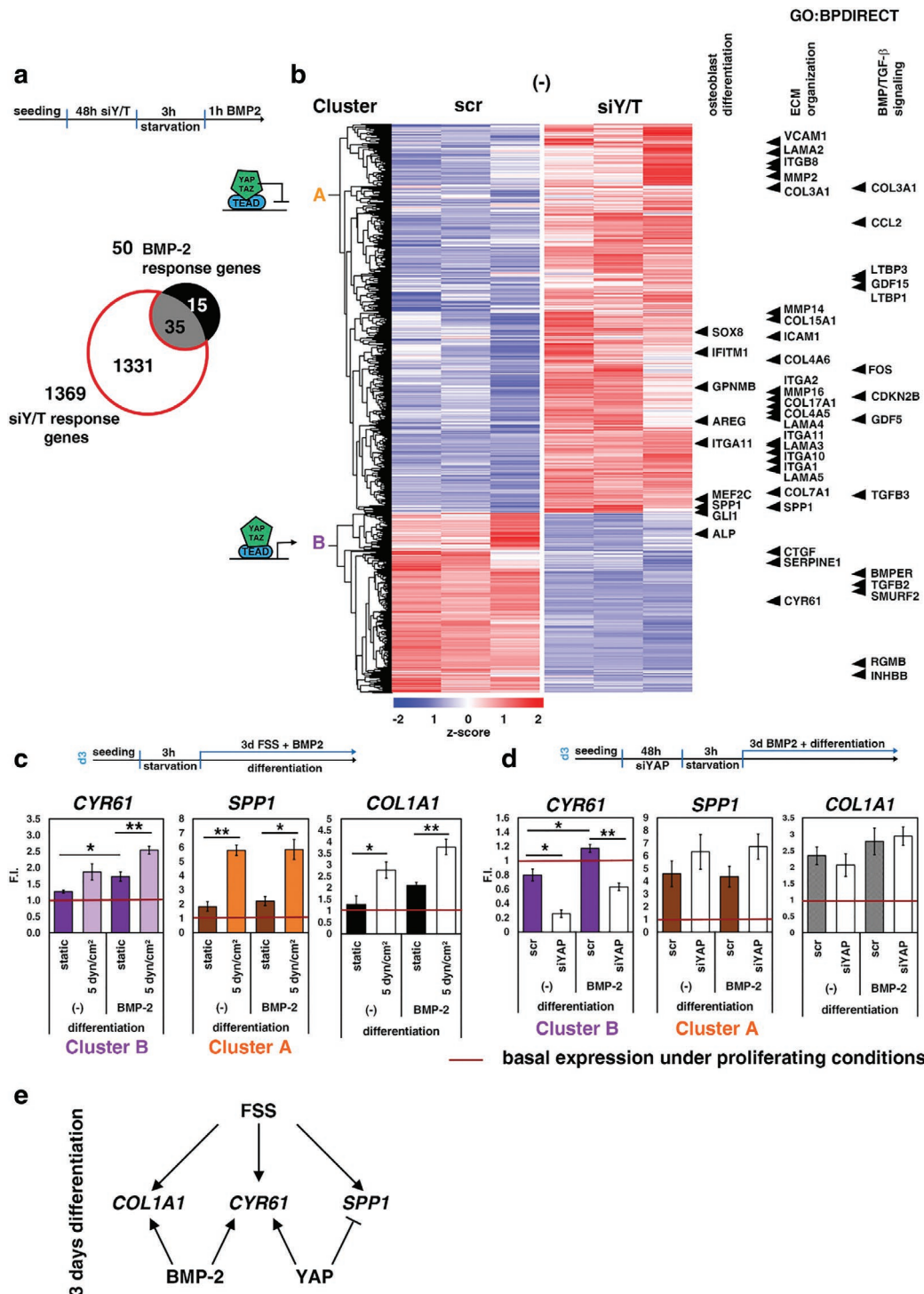
Figure 3. YAP-dependent target genes are influenced by FSS. a) Venn diagram of RNA-Seq data presenting the number of differentially expressed genes in hFOBs transfected with control siRNA and YAP/TAZ targeting siRNA (siY/T) for 48 h and afterwards stimulated with BMP-2 for 1 h. b) Hierarchical clustering of differentially expressed genes from RNA-Seq experiment (p-value < 0.05; $-0.6 \leq \log2FC \geq 0.6$) of hFOBs transfected with control siRNA and YAP/TAZ targeting siRNA for 48 h and then stimulated with BMP-2. Clustering depicts genes differentially expressed in response to YAP/TAZ exclusively. Genes highlighted next to the map were revealed by functional enrichment analysis using DAVID Bioinformatics Resources 6.8.[64] c) hFOBs were starved in medium containing 2% FCS for 3 h, and then stimulated with 5×10^{-9} M BMP-2 and cultured under static conditions or 5 dyn cm^{-2} FSS differentiating (39.5 °C) conditions for 72 h. qPCR analysis of target mRNA identified by RNA-Seq (clusters A and B). d) hFOBs depleted for YAP and control cells were starved in medium containing 2% FCS for 3 h, and then stimulated with 5×10^{-9} M BMP-2 and cultured under static and differentiating (39.5 °C) conditions for 72 h. qPCR analysis of target mRNA identified by RNA-Seq (clusters A and B). Data are normalized to untreated control at proliferation conditions and presented as mean ± SEM of three independent experiments. e) FSS stimulates osteogenic BMP-2 and YAP/TAZ targets and targets shared by both pathways.

**ADVANCED
SCIENCE NEWS**
www.advancedsciencenews.com

**ADVANCED
BIOLOGY**
www.advanced-bio.com

contribution in osteogenic differentiation. CYR61 (cluster B; Figure 3b) is positively regulated by FSS and BMP-2 stimulation as well as YAP (Figure 3c), as confirmed by depletion of YAP (Figure 3d) and RNA-Seq analyses (Figure 3b; Figure S2c, Supporting Information). SPP1 is upregulated by FSS but not by BMP-2 (Figure 3c), while YAP represses SPP1 under differentiation conditions (Figure 3d). COL1A1 encodes the major osteogenic matrix protein and is cooperatively increased by FSS and BMP-2 stimulation (Figure 3c) and is independent of YAP (Figure 3b,d). This suggests that while all three genes are upregulated by FSS, there exists a clear separation of those genes, which are BMP-sensitive (e.g., COL1A1), those which are YAP/TAZ-sensitive (e.g., SPP1) and those, which are both (CYR61); (Figure 3e). We conclude that YAP/TAZ has a distinct impact on bone matrix formation, which only in part overlaps with BMP2-signaling and that FSS has the potential to override these regulations to some extent. Furthermore, FSS and BMP-2 induce a bone specific matrix under differentiating conditions independent of YAP/TAZ signaling.

## 2.3. Classification of YAP/TAZ and/or SMAD1/5 Target Genes

BMP-activated SMADs have been previously shown to interact with YAP/TAZ to regulate target gene transcription.[46] Based on this, we hypothesized that SMAD1 and YAP/TAZ form a transcriptional complex in hFOBs. By using a proximity ligation assays (PLA), we demonstrated that SMAD1 and YAP/TAZ interact both in the cytosol and in the nucleus (**Figure 4**a). Interestingly, nuclear complexes of SMAD1 and YAP/TAZ were significantly enriched after BMP-2 stimulation (Figure 4a,b), suggesting a nuclear accumulation of transcription factor complexes composed of both proteins. On the other hand, treatment with the actin-disrupting agent cytochalasin D (CytoD) prevented the BMP-induced increase of nuclear SMAD1-YAP/TAZ interactions (Figure 4a,b), due to a retention of YAP/TAZ in the cytoplasm (Figure S3c, Supporting Information) (CytoD, latrunculin B (LatB)). With this, we conclude that SMAD1 might form a transcriptional complex with YAP/TAZ that is distinct from the classical pSMAD1-SMAD4 complexes, to regulate gene expression cooperatively. Within the 50 BMP target genes identified by RNA-Seq, 35 were also regulated by YAP/TAZ (Figure 4c) (red frame). Interestingly, 28.5% of these genes belong to the Gene Ontology (GO) cluster "osteoblast differentiation" and include, for example, NOG, JUNB, and GADD45B (Figure 4d). In a hierarchical cluster analysis of all 50 identified BMP target genes, the YAP/TAZ-dependent BMP target genes were subgrouped into clusters C, E, and F (Figure 4d). Clusters C and E represent BMP-induced genes, which are repressed by YAP/TAZ depletion. Cluster C comprises four BMP targets, which loose BMP responsiveness in the absence of YAP/TAZ, i.e., they are highly YAP/TAZ dependent. Interestingly, NOG encoding the BMP antagonist noggin is one of those four genes. Cluster E (six genes) includes BMP target genes, which are rather less affected by loss of YAP/TAZ. Among those targets is, for example, the growth arrest and DNA damage inducible beta (GADD45B), which was previously reported to regulate osteogenic differentiation.[65,66] Cluster D represents 15 BMP target genes, which are not affected by loss of YAP/TAZ (Figure 4d).

Here, we found, for example, the ID genes (ID1–3), suggesting that these are not directly influenced by the mechanotransducer YAP/TAZ. Cluster F encompasses 25 genes that are upregulated by both BMP-2 and loss of YAP/TAZ. These genes include junB (JUNB) and early growth response 2 (EGR2) encoding the mechanoresponsive transcription factors and EGR2 (Figure S4, Supporting Information). As these genes are repressed by YAP/TAZ, we consider their regulation to be independent of a transcriptional complex composed of SMAD1 and YAP/TAZ. In order to substantiate that SMAD1 directly regulates the target genes proposed earlier, we investigated SMAD1 binding loci using chromatin immunoprecipitation followed by DNA sequencing (ChIP-Seq) and compared it to RNA-Seq clustering analysis. Analysis of SMAD1 enrichment in proximity (15 kb) to the transcription start site (TSS) of 50 BMP regulated genes demonstrates that the genes classified in cluster D are strongly SMAD1 bound, whereas cluster C, E, and F genes show weak or no SMAD1 enrichment (Figure 4d). In line with this, genome browser view of ID1 and ID2 locus shows strong peaks around the TSS, whereas for, e.g., NOG, EDN1, and GADD45B, weak or no peaks are observed (Figure 4e; Figure S4b, Supporting Information) around the TSS. These results recapitulate the observations from RNA-Seq, as BMP/SMAD1-induced expression of those genes is rather low (Figure S4a, Supporting Information).
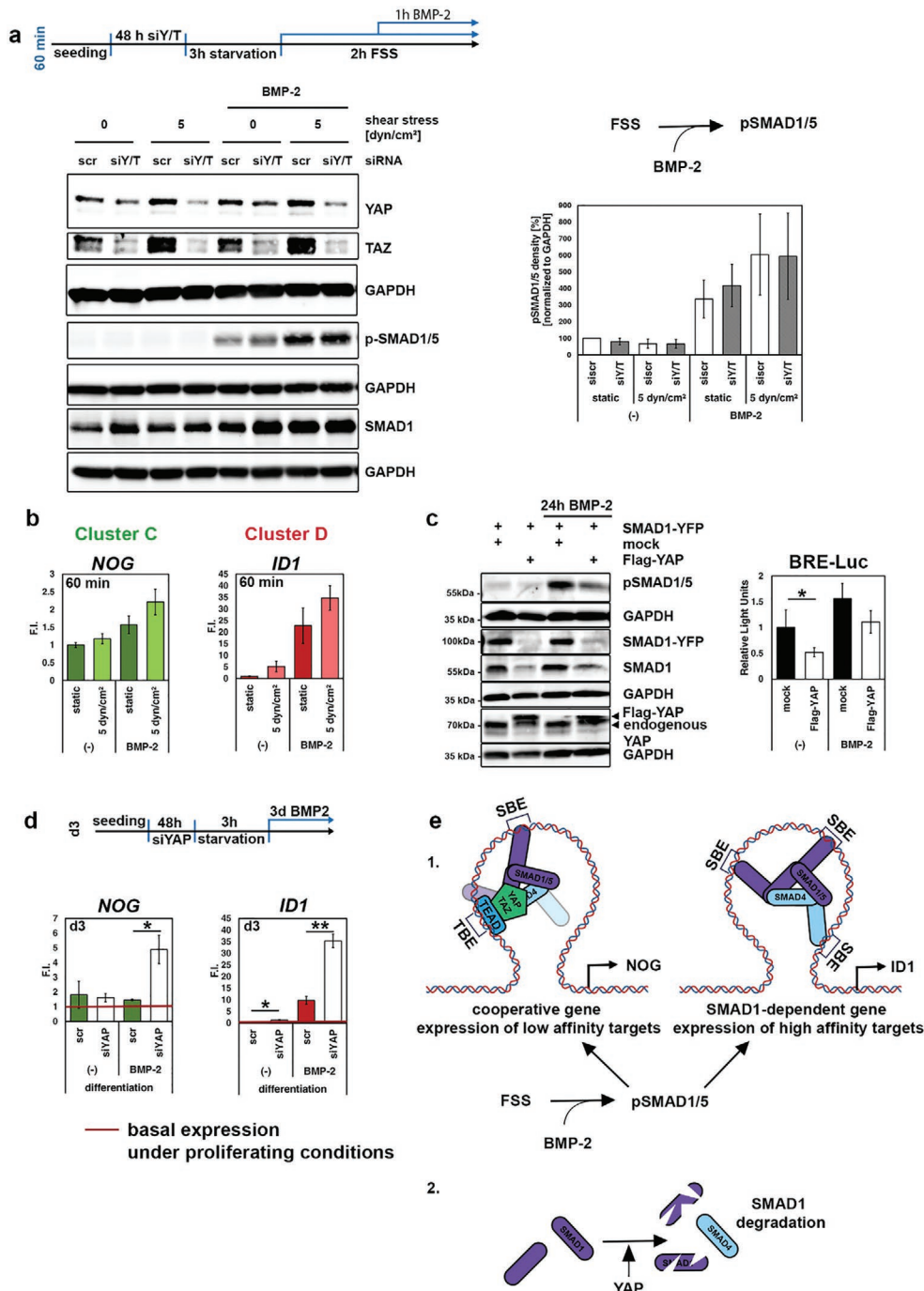
Since genes of clusters C and E are downregulated upon YAP/TAZ depletion, we further predicted TEAD-binding sites in the respective loci in silico utilizing the cis-element finder CISTER (Figure S4c, Supporting Information).[69] Here, the cis-element finder identified two TEAD cis-elements in the NOG locus, whereas the ID1 locus comprises no TEAD elements. The GADD45B locus carries one TEAD cis-element. Analysis of ChIP-Seq data from astrocytoma cell line[70,71] supported this observation, since YAP and TEAD1 show DNA occupation in the NOG, EDN1, and GADD45B but not in the ID1 gene. Collectively, these data suggest that expression of weak SMAD1 bound genes is enhanced by additional binding of YAP/TAZ, whereas some BMP target genes such as ID1–3 are independent from YAP/TAZ-based mechanotransduction.

2.4. The Impact of Mechanical Cues and pSMAD1/5 Is Different on NOG as Compared to the ID Genes

The BMP-SMAD pathway has been shown to be mechanoresponsive at different levels of the signaling cascade.[59,72,73] Thus, we analyzed SMAD1/5 signaling in response to BMP-2 under FSS conditions at different levels of the cascade. SMAD1/5 phosphorylation was dependent on BMP-2 and enhanced by FSS; however, FSS alone did not increase SMAD1/5 phosphorylation (**Figure 5**a; Figure S5a, Supporting Information). At this point, we asked whether this enhancement by FSS upon BMP-2 stimulation was mediated by YAP/TAZ: while siRNA-mediated depletion of YAP/TAZ tends to increase both SMAD1 total protein level and SMAD1/5 phosphorylation under static conditions, FSS-induced enhancement of SMAD1/5 phosphorylation was YAP/TAZ independent (Figure 5a). Here, we can exclude that this FSS-induced effect depends on endocytosis since inhibiting endocytosis with dynasore did not abolish the effect (Figure S5b, Supporting Information). Second, we
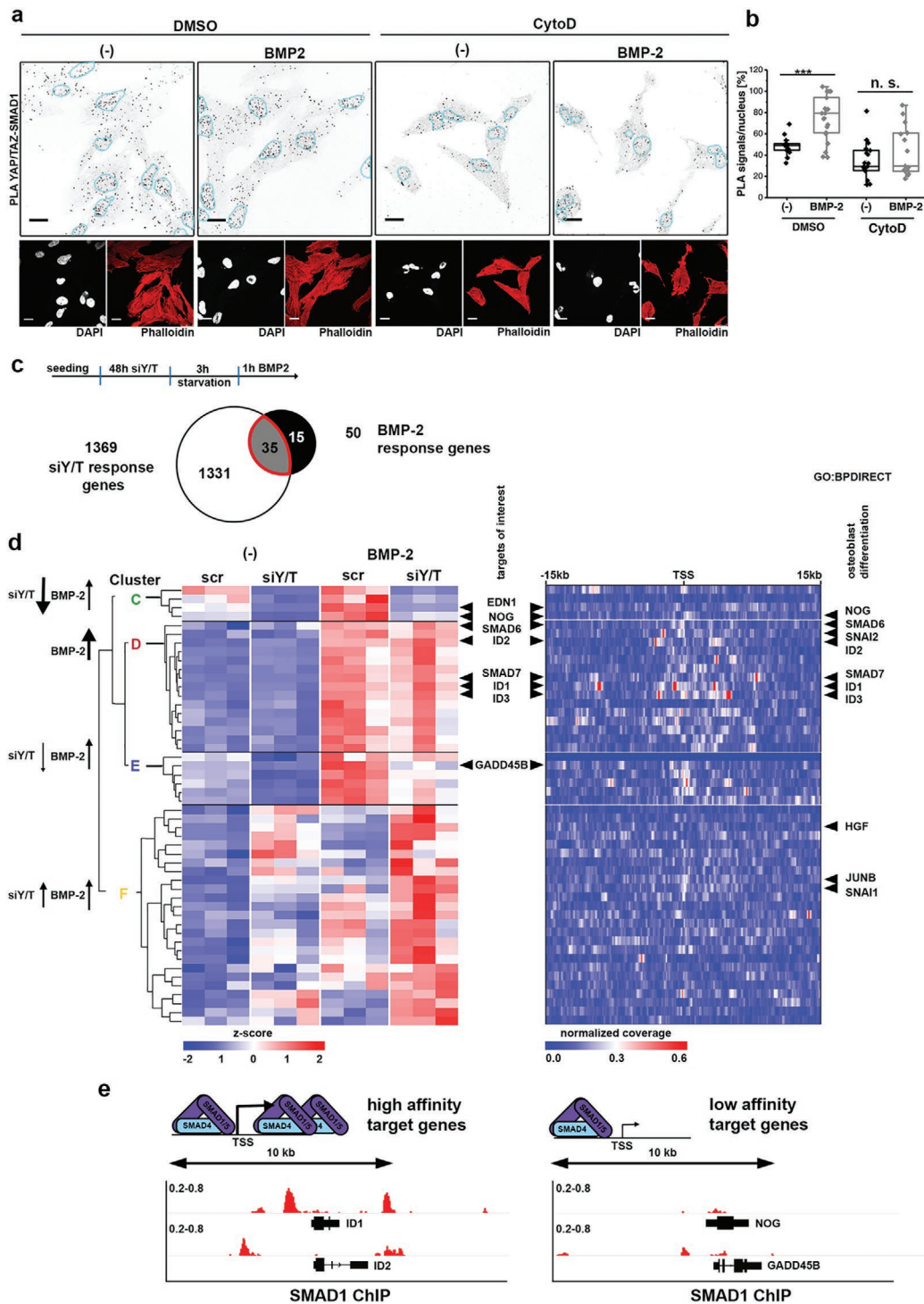
Figure 4. YAP/TAZ interacts with SMAD in an actin cytoskeleton-dependent manner, thereby influencing specific BMP target genes. a) PLA of Smad1 and YAP/TAZ in hFOBs treated with 0.4×10^{-6} M CytoD or equal volume of DMSO for 1 h, followed by stimulation with 5×10^{-9} M BMP-2 for 1 h with quantification of nuclear ligation events. b) Quantification of PLA signals per nuclei. c) Venn diagram of RNA-Seq data presenting the number of differentially expressed genes in hFOBs transfected with control siRNA and YAP/TAZ targeting siRNA for 48 h and afterwards stimulated with BMP-2 for 1 h. d) On the left, hierarchical clustering of differentially expressed genes from RNA-Seq experiment (p-value < 0.05; $-0.6 \leq$ logFC ≥ 0.6), depicting differentially expressed genes upon BMP-2 stimulation. Gene Ontology revealed genes functionally related to osteoblast differentiation. Genes highlighted next to the map were revealed by functional enrichment analysis using DAVID Bioinformatics Resources 6.8.[64] On the right, On the right, heatmap depicting normalized coverage of SMAD1-binding sites from chromatin immunoprecipitation followed by sequencing experiment (-15 kb < TSS < 15 kb) upon BMP-2 stimulation for 90 min. Heatmap was created with deeptools using the galaxy platform.[67,68] e) Genomic loci of ID1, ID2, NOG, and GADD45B are shown together. The direction of transcription of the gene is indicated by the arrow beginning at the TSS.

**ADVANCED
SCIENCE NEWS**

www.advancedsciencenews.com

**ADVANCED
BIOLOGY**

www.advanced-bio.com

Figure 5. FSS enhances BMP-2-induced SMAD1/5 phosphorylation and target gene transcription, whereas YAP inhibits BMP-induced SMAD signaling. a) Representative western blot analysis of pSMAD1/5 in hFOBs transfected with control siRNA (scr) or siRNAs targeting YAP and TAZ (siY/T) for 48 h, pre-treated with 5 dyn cm⁻² FSS and stimulated with 5×10^{-9} M BMP-2 for 1 h under static or FSS conditions and densitometric analysis of three independent experiments. b) qPCR analysis of NOG and ID1 mRNA (clusters C and D) in hFOBs pretreated with 5 dyn cm⁻² FSS and stimulated with 5×10^{-9} M BMP-2 for 1 h under static or FSS conditions. c) Left: hFOBs were transfected with SMAD1-YFP and either β-galactosidase expression vector as a control (mock) or Flag-YAP expression vector. Representative western blot shows pSMAD1/5 and total SMAD1 level when overexpressing Flag-YAP and stimulated with BMP-2 for 24 h. Right: Dual luciferase assay of hFOBs transfected with BRE-Luc reporter, pRL-TK control vector, and either β-galactosidase expression vector as a control (mock) or Flag-YAP expression vector. Cells were starved for 6 h and then stimulated with 5×10^{-9} M BMP-2 for 24 h. Relative light units are presented as mean ± SD of five independent experiments. *$p < 0.05$, two-way ANOVA with Bonferroni post hoc test, compared to corresponding mock-transfected control. d) hFOBs depleted for YAP and control cells were starved in medium containing 2% FCS for 3 h, and then stimulated with 5×10^{-9} M BMP-2 and cultured under differentiating (39.5 °C) conditions for 72 h. qPCR analysis of target mRNA NOG and ID1 identified by RNA sequencing (clusters C and D). Data are normalized to untreated control under proliferation conditions and presented as mean ± SEM of three independent experiments. e) Schematic illustration depicting the inhibitory effect of YAP/TAZ on pSMAD1/5 and subsequent SMAD1/5-dependent target gene expression.

**ADVANCED
SCIENCE NEWS**
www.advancedsciencenews.com

**ADVANCED
BIOLOGY**
www.advanced-bio.com

analyzed transcription of selected genes (clusters C, D, and E) that we have identified as YAP/TAZ and BMP-dependent genes in response to FSS and BMP-2 stimulation, after short-term proliferating (Figure 5b) and long-term differentiating conditions (Figure S5c, Supporting Information). Here, expression of NOG, ID1, ID2, and GADD45B was enhanced by FSS and BMP-2 stimulation in a cooperative manner, possibly as a consequence of enhanced SMAD1/5 phosphorylation (Figure 5b; Figure S5c,d, Supporting Information). Of note, induction of NOG by BMP-2 is ten times lower when compared to the ID genes, highlighting a requirement for high SMAD1/5 phosphorylation levels (Figure 5b). Interestingly, both short-term (2 h) and long-term (3 days) FSS stimulation similarly enhance BMP-2-induced NOG expression, even though the YAP activation status is different (Figures 1 and 2). This suggests that FSS regulation of BMP target genes is primarily dependent on changes in the level of SMAD1/5-phosphorylation rather than on YAP/TAZ. Since short-term FSS-dependent enhancement of SMAD1/5 phosphorylation was YAP/TAZ independent, we checked whether long-term YAP/TAZ activation, as seen by FSS, alters SMAD1/5 phosphorylation. For this, we overexpressed YAP and measured both SMAD phosphorylation (Figure 5c, left) and SMAD-reporter gene activity (BRE-luc; Figure 5c, right; expression controls in Figure S5f, Supporting Information). Under both basal and BMP-2 stimulation conditions, overexpression of YAP resulted in a decrease of SMAD1/5 phosphorylation (Figure 5c, left) and reporter gene activity (Figure 5c, right). However, this effect was due to SMAD1 degradation, as seen for both the endogenous SMAD (Figure 5c, right, panel 4 from bottom) and for coexpressed SMAD-YFP (Figure 5c, right, panel 5 from bottom), indicating a mechanism independent of transcription. This suggests that YAP/TAZ has probably multiple ways to crosstalk with BMP-SMAD signaling. This was most strikingly evident for NOG and ID1 expression, when YAP/TAZ was depleted under 3D differentiation conditions, whereas ID1 expression is strongly enhanced, induction of NOG by BMP2 is only seen when YAP/TAZ were depleted from cells (Figure 5d). This effect is explained by higher pSMAD1/5 level in the absence of YAP.

Taken together, our data identify NOG as a gene, only induced when high amounts of phosphorylated SMAD1/5 are available. This is achieved through BMP-2 plus FSS costimulation, as both signals cooperatively increase the levels of pSMADs (Figure 5a) but also under conditions, where BMP-2-mediated SMAD1 signaling is not disturbed by the mechanosensor YAP/TAZ (Figure 5d). On the contrary, the FSS-dependent regulation of ID1 (Figure 5b) and ID2 (Figure S5c, Supporting Information) is not affected by depletion of YAP/TAZ (shown by RNA-Seq, Figure 4d), making the ID genes solely dependent on pSMAD1/5 (Figure 4d) but independent of YAP/TAZ transcriptional activity. Our data here show that FSS enhance BMP-2-induced pSMAD1/5 independent of YAP/TAZ subsequently activating BMP-dependent and cooperative target genes (Figure 5e). By an independent process, YAP promotes SMAD1 degradation, which in turn decreases the level of phosphorylated SMAD1/5 and its target gene transcription. This further supports the concept that BMP-2 efficiency in osteogenic differentiation is largely dependent on mechanical inputs and crosstalk from mechanosensors, such as YAP/TAZ.

2.5. YAP/TAZ- and TGF-β-Induced SMAD2/3 Target Gene Expression Is Influenced by FSS and Osteogenic Differentiation

Not only BMPs influence osteogenic differentiation, but also TGF-β.[74] Thus, we asked whether TGF-β-SMAD2/3 signaling is also affected by YAP and FSS. FSS enhanced TGF-β-induced SMAD2 phosphorylation and subsequently TGF-β-dependent target gene expression (e.g., CTGF and GADD45B; **Figure 6**a,b). Apart from that, SMAD2 phosphorylation is decreased after 3 h of TGF-β treatment in YAP/TAZ-depleted cells, whereas the initial SMAD2 phosphorylation is unaffected (Figure 6c). Next, we analyzed TGF-β target genes CTGF and GADD45B and osteogenic marker gene expression of ALP, SPP1, and COL1A1 (Figure 6d). Accordingly, all those genes are induced by TGF-β, whereby expression of ALP, CTGF, and GADD45B is clearly YAP dependent. Analyzing ChIP-Seq experiments from astrocytoma and breast cancer cells revealed that SMAD3 and YAP/TEAD occupy regulatory regions in the GADD45B and CTGF loci (Figure S4b, Supporting Information), suggesting a cotranscriptional activity of YAP and SMAD2/3. In contrast, YAP depletion further increases SPP1 and COL1A1 expression. Since COL1A1 is a YAP-independent target (Figure 3b,e), the observed increase is likely a consequence of YAP-dependent regulation of SMAD2/3 signaling rather than a YAP transcriptional effect. Altogether, we conclude that FSS elevates TGF-β-induced SMAD2/3 signaling, which cooperatively with YAP/TAZ enhances the transcription of shared target genes.

3. Conclusion

FSS occurs in bone through the interstitial fluid flow in the intramedullary space and stimulates osteoblast differentiation.[6,75] In order to characterize the molecular impact of FSS on pathway regulation and transcription in bone, we utilized an in vitro system allowing the application of FSS on osteoblasts. This enabled the detailed analysis of FSS-induced actin reorganization and transcriptional and post-translational changes during differentiation. Here, we focused on the regulation of the well-characterized mechanotransducers YAP/TAZ and their crosstalk to the BMP-2 signaling cascade, a prominent growth factor signaling pathway in bone. Therefore, we performed RNA and ChIP-Seq to identify classes of genes distinctly regulated by YAP/TAZ and BMP-2. YAP/TAZ and SMADs share target genes, which play an important role in osteogenic differentiation. Further, identified genes constitute specific markers induced upon mechanoosteogenic induction, which could be utilized as markers for the design of mechanical therapies of bone diseases like osteoporosis.

Here, we have shown that osteoblasts react to FSS by immediate actin cytoskeleton remodeling to form higher-ordered actin bundles. At this stage, YAP/TAZ is inactivated and only released for activation after long-term FSS conditions. During osteogenic differentiation, increased YAP/TAZ target gene expression was described previously.[25,26] It is remarkable that only a subset of osteogenic marker genes is susceptible to FSS (e.g., SPP1 and COL1A1) while others are unaffected (e.g., ALP), implying a distinct contribution of mechanics into osteogenic differentiation control. Here, we distinguish between FSS and
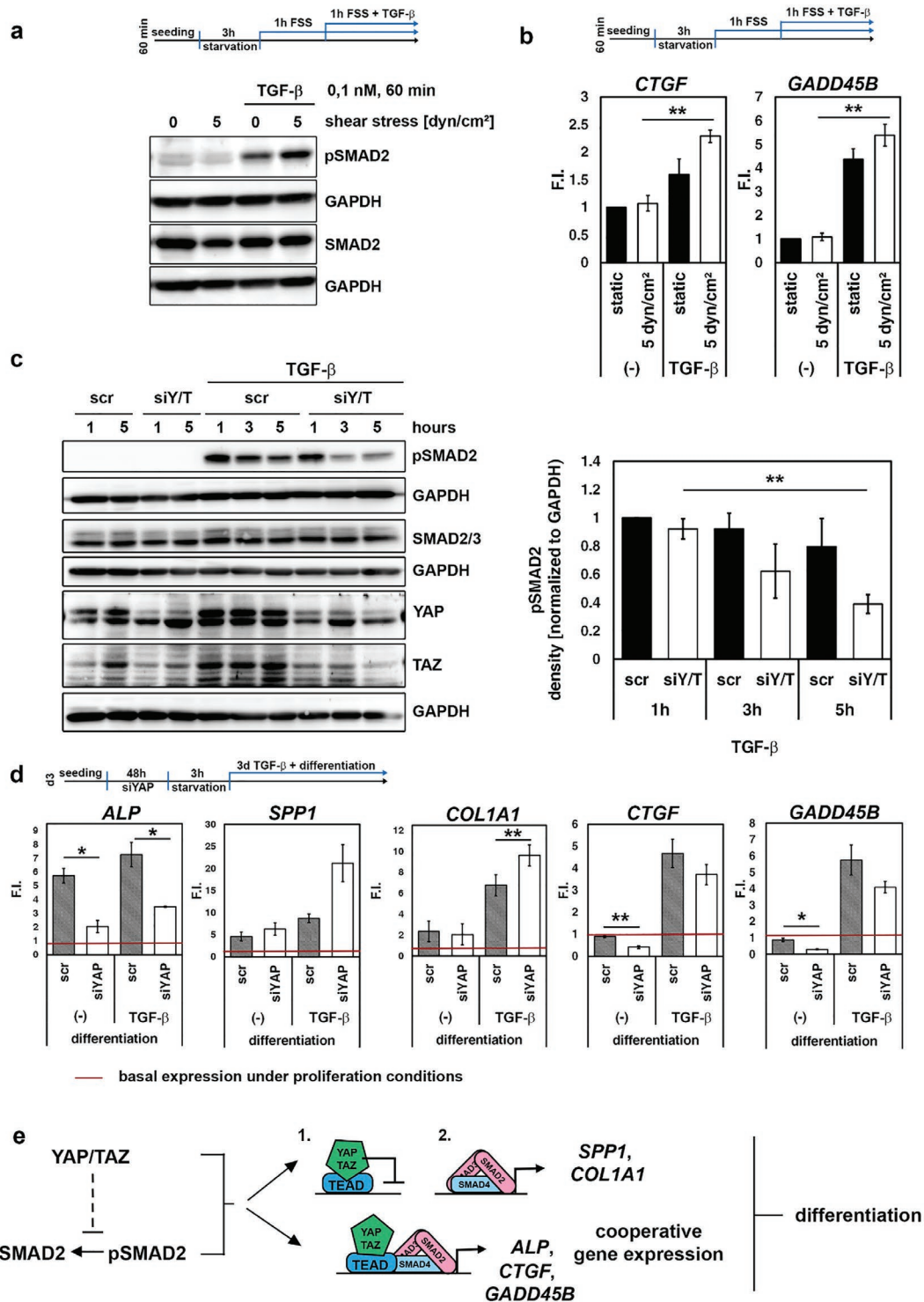
Figure 6. FSS enhances TGF-β-induced SMAD2 signaling and target gene expression and YAP/TAZ enhances TGF-β-induced SMAD2 phosphorylation. a) Representative western blot analysis of pSMAD2 in hFOBs pretreated with 5 dyn cm^{-2} FSS and stimulated with 0.1×10^{-9} M TGF-β for 1 h under static or FSS conditions. b) qPCR analysis of TGF-β-dependent target gene expression of CTGF and GADD45B in hFOBs pretreated with 5 dyn cm^{-2} FSS and stimulated with 0.1×10^{-9} TGF-β for 1 h under static or FSS conditions. c) Representative western blot analysis of hFOBs transfected with control siRNA (scr) or siRNAs targeting YAP and TAZ (siY/T) for 48 h, and then stimulated with 0.2×10^{-9} M TGF-β. Densitometric quantification of pSMAD2 normalized to GAPDH levels demonstrates a reduction in SMAD2 phosphorylation upon YAP/TAZ depletion. d) hFOBs depleted for YAP and control cells were starved in medium containing 2% FCS for 3 h, and then stimulated with 5×10^{-9} M BMP-2 and cultured under static conditions at proliferating (34 °C) or differentiating (39.5 °C) conditions for 72 h. qPCR analysis of osteogenic marker mRNA and TGF-β target gene expression. Data are presented as mean ± SEM of three independent experiments. e) Schematic illustration depicting the enhancing effect of YAP/TAZ on pSMAD2 and subsequent SMAD2-dependent target gene expression.

**ADVANCED
SCIENCE NEWS**
www.advancedsciencenews.com

**ADVANCED
BIOLOGY**
www.advanced-bio.com

YAP/TAZ as mechanical regulators and found that, for example, SPP1 expression is both sensitive to YAP/TAZ and FSS; however, FSS-mediated SPP1 is independent of YAP/TAZ. This implies that genes very susceptible to mechanical stimulation such as SPP1 are sensitive to various mechanopathways, while other osteogenic marker genes are differentially affected. YAP depletion vastly reduces transcription of the osteogenic marker ALP, suggesting that YAP/TAZ activity is required for osteogenic differentiation, which is in line with previous reports.[76–78] Of note, Xiong et al. observed that YAP/TAZ can have inducing as well as repressing effects on osteoblastic effects dependent on the differentiation stage in transgenic mice.[79] Here, depletion of YAP/TAZ in mature osteoblasts via Dmp1-Cre inhibits bone formation, whereas differentiation of osteoblastic precursors is promoted when YAP/TAZ is depleted via Prx1/Osx1-Cre. In our experiments, we observe differentiation of mature osteoblasts with regard to matrix deposition (SPP1 and COL1A1 expression) that coincides with these observations of YAP/TAZ exhibiting pro-osteogenic action at this differentiation stage.

Beside YAP/TAZ's action as co-transcription factors, Monroe et al. have shown that overexpressing constitutively active YAP results in chromatin remodeling, thereby changing the accessibility for TEAD to bind chromatin.[80] Further, YAP/TAZ was described to recruit the NuRD complex to DNA, which results in deacetylation and chromatin remodeling, consequently repressing transcription.[81] Additionally, interaction with other chromatin remodelers including SWI/SNF complex, GAGA factor, and mediator complex has been reported.[82,83] In our RNA-Seq study, we observed that the majority of YAP/TAZ-dependent genes (cluster A) was induced by their depletion, possibly due to this chromatin remodeling effect of YAP. This mode of action can also be assumed for half of the shared BMP-YAP/TAZ target genes (cluster F; Figure 4d).

To understand the impact of FSS on osteogenic differentiation, we focused on the regulation of BMP/TGF-β signaling by FSS-induced changes in YAP/TAZ activity, as osteogenesis is strongly regulated by BMP and TGF-β signaling.[84] Several studies on mechanosensitivity of BMP signaling show that mechanical inputs can be integrated into the cascade already at the level of BMP-receptor-mediated SMAD phosphorylation.[19,22,72] Using a 3D bioreactor system to cyclically load hFOBs, we previously found a cooperation between BMP-2 stimulation and mechanical loading on SMAD activation and target gene transcription.[19] We confirmed this here and show that short-term FSS stimulation enhances BMP-induced SMAD signaling in hFOBs. This increase in early SMAD phosphorylation, both for SMAD1/5 and SMAD2/3, however, is clearly independent of YAP/TAZ action, extending on the understanding of molecular mechanism proposed previously.

In our RNA sequencing experiment, we identified distinct classes of BMP target genes. NOG encoding the BMP antagonist noggin belongs to a class of BMP target genes highly dependent or susceptible to YAP/TAZ and high levels of phosphorylated SMAD1/5, thereby acting as a perfect sensor for overshooting BMP signaling, as it appears by FSS stimulation or YAP/TAZ depletion. Another class includes the ID1–3 genes, which are strongly enhanced by relatively low levels of phosphorylated SMAD1/5 but not altered by YAP/TAZ transcriptional activity, demonstrating that IDs are high-affinity

SMAD1/5 target genes. This promotes the concept that BMP-2 efficiency in osteogenic differentiation is largely dependent on mechanical inputs and crosstalk from mechanosensors, such as YAP/TAZ. Based on our study, we propose four independent modes of BMP signaling regulation by YAP/TAZ (**Figure 7**). These four modes affect either the SMAD level, their phosphorylation, or SMAD-induced target gene transcription. First, YAP/TAZ as transcriptional cofactors regulate gene expression of BMP pathway components. In vivo knockdown of YAP or TAZ in mouse models was found to reduce TGF-β1 and Smad2 expression and also Bmp4 was shown to be a target of YAP and TAZ.[85–87] In our study, we found primarily ligands, ligand-binding proteins, and the BMP coreceptor RGMB and the BMP inhibitor BMPER to be regulated by YAP/TAZ. These proteins act already at the BMP receptor level and would result in an altered SMAD1/5 phosphorylation as seen in our system. Second, BMP- and TGF-β-induced transcription is regulated by YAP/TAZ through their interaction with SMAD1/5 or SMAD2/3, consequently modulating gene expression of shared target genes (Figure 7), as shown by our RNA-Seq experiment. Analyzing cis-elements for SMAD1 and TEAD in silico[69,70,88,89] together with ChIP-Seq studies[70,71] revealed that YAP occupies regulatory regions proximal to the NOG, EDN1, and GADD45B gene locus, but SMAD1 does not or only weakly binds to these loci. Here, we propose that the IDs are high-affinity target genes that are sensitive to low phospho-SMAD1 level but their expression is not regulated by YAP/TAZ. NOG, EDN1, and GADD45B are low-affinity target genes, whose gene expression might require further transcription cofactors like YAP/TAZ or high levels of phospho-SMAD1/5 as triggered by FSS. For example, NOG is clearly dependent on both YAP/TAZ and SMADs being present in a transcriptional complex. Under conditions by which YAP/TAZ affect phospho-SMAD levels, this effect is difficult to judge. Short-term conditions, in which lack of YAP/TAZ does not affect phopho-SMAD1/5 levels (RNA-Seq, +BMP2), show clearly that both YAP/TAZ and phospho-SMAD1/5 are required for NOG induction. Enhanced levels and accumulation of pSMAD1 as seen under long-term BMP2 stimulation (24 and 72 h) and YAP/TAZ knockdown show induction of NOG (Figure 5d). This clearly suggests that the expression level of NOG is a measure of high pSMAD1 levels in a cell, while other targets such as ID1 have a very different threshold and react already at much lower pSMAD1/5 levels. We also confirmed TGF-β targets, i.e., CTGF and GADD45B, to be YAP/TAZ dependent. Hiemer et al. described that TGF-β-mediated CTGF expression requires YAP/TAZ-TEAD interacting with SMAD2/3 in a transcriptional complex in breast cancer cells.[90] Thus, the observed loss of CTGF and GADD45B expression upon YAP depletion could be caused by the lack of YAP/TEAD interaction with SMAD2/3 at respective regulatory regions.

Third, YAP/TAZ potentially targets SMAD1 for degradation in the cytosol, what might explain increased SMAD1 levels and SMAD-only target gene expression upon YAP/TAZ depletion (Figure 7). Here, it must be emphasized that this regulation manifests over long-term BMP2 stimulation. In contrast, stimulating YAP/TAZ-depleted cells for a short time period resulted in a marginal increase in SMAD1/5 phosphorylation and did not alter SMAD-only targets like the ID genes.
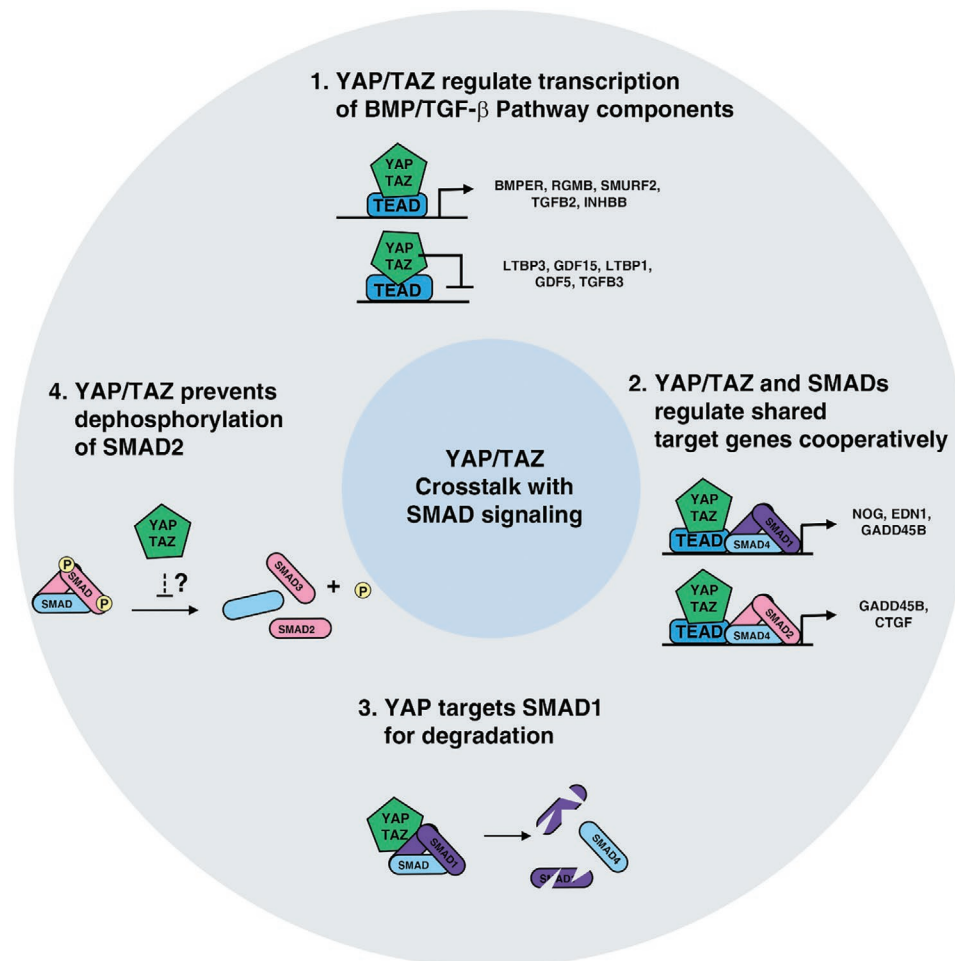
Figure 7. Schematic illustration of the four modes shows how YAP/TAZ impacts BMP and TGF-β induced SMAD signaling.

Summarizing, YAP/TAZ negatively regulate BMP signaling, confirming earlier reports.[91] On the other hand, it was also described that YAP/TAZ interact with SMAD1 at the linker region to prevent its proteasomal degradation.[46] In our cell system, we could not substantiate this, as YAP/TAZ depletion results in increased SMAD1 levels. Fourth, in contrast to the impact of YAP/TAZ on BMP signaling, YAP/TAZ depletion reduces TGF-β-SMAD2 phosphorylation. This occurred after 3 h of TGF-β stimulation, while initial phosphorylation was not affected. As SMAD2/3 level was not altered, we assume that this effect is mediated by a YAP/TAZ-dependent phosphatase. In conclusion, we have shown that YAP/TAZ influences BMP/TGF-β-SMAD-dependent signaling through different mechanisms including SMAD degradation, dephosphorylation, and distinct transcriptional complex formation.

Bone homeostasis and efficient regeneration of fractures and defects depend on proper osteogenic differentiation of progenitor cells.[92] In aged patients, bone becomes brittle and regenerative capacity decreases, resulting in aging-associated diseases like osteoporosis.[93,94] The connection between FSS, YAP/TAZ, and BMP/TGF-β signaling crosstalk and osteogenic differentiation of bone progenitor cells uncovered in this study might, therefore, constitute a target for novel therapies treating age-associated bone frailty. Thereby, we recommend NOG, GADD45B, and CTGF as target genes, which can be monitored to evaluate BMP/TGF-β and mechanically induced osteogenic differentiation in therapeutic and screening approaches.

4. Experimental Section

Cell Culture: hFOB cells (cell line hFOB 1.10, ATCC CRL-11372) were cultured in a 1:1 mixture of Dulbecco's modified Eagle's medium (DMEM) and Ham's F12 medium with 2.5×10^{-3} M L-glutamine and 8.1 mg L^{-1} phenol red (Thermo Fisher Scientific, Waltham, USA) supplemented with 10% fetal calf serum (FCS, Biochrom AG, Berlin, Germany) and antibiotics (100 U mL^{-1} penicillin and 0.1 mg mL^{-1} streptomycin, PAN-Biotech GmbH, Aidenbach, Germany, and 0.3 mg mL^{-1} G418, Biochrom AG). The cells were grown at a permissive temperature of 33.5 °C[62] in a 5% CO$_2$ humidified atmosphere for expansion and experiments analyzing non-differentiating cells.

Growth Factor Stimulation, Toxin Treatment, and Osteogenic Differentiation: Actin fibers were destabilized with CytoD (Enzo Life Sciences GmbH, Lörrach, Germany) and LatB (Merck KGaA, Darmstadt, Germany). DMSO (Carl-Roth GmbH, Karlsruhe, Germany) was used as a control. BMP-2 was a generous gift by Prof. W. Sebald (Biozentrum Universität Würzburg, Würzburg, Germany). TGF-β was obtained from Peprotech (Hamburg, Germany). Generally, cells were starved for 4 h

**ADVANCED
SCIENCE NEWS**

www.advancedsciencenews.com

**ADVANCED
BIOLOGY**

www.advanced-bio.com

in media without FCS and then stimulated with 5×10^{-9} M BMP-2 or 200×10^{-12} M TGF-β for 1 h, unless otherwise noted. For osteogenic differentiation, cells were starved in media containing 2% FCS for 3 h and then cultured at either 33.5 °C as a control or at a restrictive temperature of 39.5 °C to induce spontaneous differentiation. Human FOBs were immortalized by Harris et al. using a temperature-sensitive mutant of the SV40 large T antigen that is active at the permissive temperature of 33.5 °C, leading to rapid cell division. At the restrictive temperature of 39.5 °C, the antigen is inactivated, proliferation stops, and the cells start to undergo spontaneous osteogenic differentiation.[62]

siRNA-Mediated Knockdown: To deplete YAP and TAZ, cells were transfected with ON-TARGETplus SMARTpool human siRNA targeting YAP1 or WWTR1 (L-012200-00-0005 and L-016083-00-0005, Dharmacon, Lafayette, USA). Cells were transfected with a final siRNA concentration of 50×10^{-9} M using Lipofectamine RNAiMAX (Thermo Fisher Scientific). Cells were analyzed 48 h post-transfection to ensure efficient knockdown.

Flow Stimulation: For shear stress experiments, hFOBs were seeded in flow chamber slides (ibidi GmbH, Martinsried, Germany). Static controls were seeded in dummy flow chambers glued on cell culture dishes. Cells were cultured for 48 h in these chambers, whereby medium was exchanged twice per day for proper nutrition supply. Laminar flow with a magnitude of 5 dyn cm^{-2} (0.5 Pa) was applied using the ibidi pump system device (Figure S1, Supporting Information) (ibidi GmbH) assembled in the cell culture incubator. Static control samples were treated with the same amount of medium as flow-treated samples after removing dummy flow chamber.

Immunofluorescence Staining: For immunofluorescence stainings, cells were fixed using 4% paraformaldehyde for 10 min and were permeabilized in 0.1% Triton X-100 for 10 min. After blocking with 3% bovine serum albumin (BSA, Carl-Roth GmbH, Karlsruhe, Germany) in PBS for 1 h, the cells were incubated with Phalloidin CruzFluor 594 (1:1000, Santa Cruz Biotechnology, Dallas, USA) overnight at 4 °C. Nuclei were counterstained with DAPI (Sigma-Aldrich, St. Louis, USA) for 5 min prior to microscopy at a Zeiss Axiovert 200M epifluorescence microscope.

In Situ PLA: For PLA, cells were plated on glass coverslips. Treated cells were fixed with 4% paraformaldehyde and permeabilized in 0.5% Triton X-100. PLA was performed using the Duolink in situ PLA technology (Sigma-Aldrich) according to the manufacturer's instruction, using anti-SMAD1 XP rabbit mAb (#6944, Cell Signaling Technology, Danvers, USA), anti-YAP/TAZ mouse mAb (sc-101199, Santa Cruz Biotechnology), and anti-SMAD4 mouse mAb (sc-7966, Santa Cruz Biotechnology) at a 1:200 dilution. Slides were mounted using Fluoromount-G (Southern Biotech, Birmingham, USA) and imaged using a Leica TCS SP8 confocal microscope.

Quantitative Real-Time PCR: Cellular RNA was isolated using the NucleoSpin RNA isolation kit (Macherey-Nagel, Düren, Germany) according to the manufacturer's instructions. 0.5 to 1 µg total RNA was reversely transcribed by incubating it with random primers (100 pmol µL^{-1}, Invitrogen, Carlsbad, USA) and M-MuLV reverse transcriptase enzyme (200 000 U mL^{-1}, New England Biolabs, Ispwich, USA) were added per sample. RT-PCR was performed using a StepOnePlus Real-Time PCR System (Thermo Fisher Scientific) with specific primers for the genes listed in Table S1, Supporting Information. Reactions were performed in triplicates in MicroAmp Optical 96-well reaction plates (Thermo Fisher Scientific) using SYBR Green PCR Master Mix (Invitrogen) or Luna PCR Master Mix (New England Biolabs). Fold induction was calculated by comparing relative gene expression to the housekeeping gene RSP9 using the ΔΔCT method.

RNA-Seq Experiment: For each experimental condition, three biological replicates were analyzed. After initial quality control using Agilent's Bioanalyzer, sequencing libraries were prepared from 500 ng of total RNA per sample following Roche's stranded "KAPA RNA HyperPrep" library preparation protocol for single indexed Illumina libraries: First, the polyA-RNA fraction was enriched using oligo-dT-probed paramagnetic beads. Enriched RNA was heat-fragmented and subjected to first strand synthesis using random priming. The second strand was synthesized incorporating dUTP instead of dTTP to

preserve strand information. Afterwards, A-tailing Illumina sequencing compatible adapters were ligated. Following bead-based clean-up steps, the libraries were amplified using ten cycles of PCR. Library quality and size was checked with qBit, Agilent Bioanalyzer and qPCR. Sequencing was carried out on an Illumina HiSeq 4000 system in PE75bp mode yielding between 15 and 23 million fragments per sample.

RNA-Seq Data Analysis: Following base calling, data were mapped against the GRCh38 genome obtained from http://emea.support.illumina.com/sequencing/sequencing_software/igenome.html using STAR v2.5.3a (STAR: ultrafast universal RNA-Seq aligner). To find differentially expressed genes, a TMM normalization of the read count data was applied and the resulting cpm values were used for GLM-based testing with edgeR.[95] Genes with a logarithmic fold change smaller than $-0.6\leq$ and bigger than ≥0.6 and p-value < 0.05 (genes with cpm < 3 were excluded) were considered to be significantly differentially expressed. For heatmaps, z-score of these genes was used and hierarchically clustered using RStudio. Clusters were identified by visual inspection. Functional enrichment and clustering was performed using DAVID Bioinformatics Resources 6.8.[64] Functional clusters with Bonferroni corrected p-value ≤ 0.05 were considered as significant.

Chromatin Immunoprecipitation Followed by Next-Generation Sequencing (ChIP-Seq): For chromatin immunoprecipitation followed by next-generation sequencing (ChIP-Seq), cells were grown to confluence and then starved in 0% FCS for 3 h and stimulated with BMP-2 (5×10^{-9} M) for 90 min. Cells were fixed in 1% formaldehyde and quenched by adding glycine 125×10^{-3} M for 5 min at 4 °C. After this, cells were harvested and lysed according to the protocol described by Lee et al.[96] and chromatin was sheared by sonication using the Bioruptor ultrasonicator (Diagenode). Sheared chromatin was immunoprecipitated using 10 µg of total SMAD1 antibody (Cell Signaling, #9743) or the normal rabbit IgG antibody (Cell Signaling, #2729) as a control, followed by incubation with protein G magnetic beads (Invitrogen). DNA was eluted in elution buffer[96] and DNA purification was performed by using DNA purification buffers and spin columns kit, according to the manufacturer's instructions (Cell Signaling).

Sequencing data quality was assessed prior to processing using FastQC (version 0.11.8). Quality trimming and adapter clipping was performed using cutadapt (v.2.4) with the following parameters: minimum length = 25, minimum quality = 20, overlap = 5, followed by a quality assessment using FastQC. Trimmed reads of enriched and input samples were aligned to GRCh38 using BWA-MEM and sorted using SAMtools v.1.10. BAMStats were used to monitor the alignment statistics. Duplicate reads were removed using GATK4/Picard MarkDuplicates (v.4.1.4.1). Reads with a mapping quality of below 15 were filtered using SAMtools view. Genome-wide bigWig coverage files were created using bamCoverage 3.4.3 without data normalization and with CPM normalization for enriched and input samples. Peak calling was performed using macs 2.1 for broad and narrow peaks on the enriched and corresponding input samples as control. Background was subtracted using macs2 bdgcmp. After completion of all steps, multiQC was applied to gather and compare all quality control results. RNA-Seq and ChIP data are published on gene expression omnibus with accession number GSE137035.

Western Blot: Cells were lysed in Laemmli buffer[97] and boiled at 95 °C for 5 min prior to separation on 10–12.5% SDS–PAGE gels. Proteins were transferred onto nitrocellulose membranes (neoLab Migge Laborbedarf-Vertriebs GmbH, Heidelberg, Germany). Membranes were blocked in 5% w/v BSA (Sigma-Aldrich) in TBST and then incubated with primary antibodies diluted 1:1000 overnight at 4 °C. The next day, membranes were incubated with goat-α-rabbit-HRP or goat-α-mouse-HRP secondary antibodies (1:10 000, Dianova, Hamburg, Germany), prior to detection with WesternBright Quantum ECL HRP substrate (advansta, Menlo Park, USA) using a Fusion-FX7 (Vilber Lourmat, Eberhardzell, Germany). Primary antibodies used were anti-GAPDH rabbit mAb (#2118, Cell Signaling Technology), anti-phospho-SMAD1/5 (Ser463/465) rabbit mAb (#9516, Cell Signaling Technology), anti-SMAD1 XP rabbit mAb (#6944, Cell Signaling Technology), anti-phospho-LATS1 (Thr1079) rabbit mAb (#8654, Cell Signaling Technology), anti-phospho-Smad2 (Ser465/467)

rabbit mAb (#3108 Cell Signaling Technology), anti-SMAD2 rabbit mAb (#3122, Cell Signaling Technology), and anti-YAP/TAZ mouse mAb (sc-101199, clone 63.7, Santa Cruz Biotechnology). Western blots are representative of at least three individual repetitions.

Dual Luciferase Assay: The cells were transfected with BMP-responsive element firefly luciferase reporter plasmid (BRE-Luc[98]), constitutively expressed *Renilla* luciferase plasmid (RLTK, Promega, Madison, USA), and Flag-YAP expression plasmid or β-galactosidase expression plasmid as control using Lipofectamine 2000 (Thermo Fisher Scientific). The next day, cells were starved for 3 h in media containing 0.5% FCS and then stimulated with 5×10^{-9} M BMP for 24 h. Cells were lysed in passive lysis buffer (Promega) and firefly and *Renilla* luciferase activities were measured using an Infinite 200 PRO plate reader (Tecan, Männedorf, Switzerland) according to the Dual-Luciferase reporter assay system protocol (Promega). Relative light units for each condition were calculated by normalizing firefly luciferase activity to *Renilla* luciferase activity. To confirm expression of YAP-Flag, lysate of each well from the triplicates was pooled and analyzed by SDS–PAGE and western blotting.

Statistics: All experiments were performed at least three times. Two-way analysis of variance (ANOVA) with Bonferroni post hoc test was performed for comparisons of multiple groups. A *p*-value lower than 0.05 was considered statistically significant.

Supporting Information

Supporting Information is available from the Wiley Online Library or from the author.

Conflict of Interest

The authors declare no conflict of interest.

[1] S. J. Mellon, K. E. Tanner, *Int. Mater. Rev.* **2012**, *57*, 235.
[2] W. Bonfield, P. K. Datta, *J. Biomech.* **1974**, *7*, 147.
[3] T. H. Ambrosi, A. Scialdone, A. Graja, S. Gohlke, A.-M. Jank, C. Bocian, L. Woelk, H. Fan, D. W. Logan, A. Schürmann, L. R. Saraiva, T. J. Schulz, *Cell Stem Cell* **2017**, *20*, 771e6.
[4] N. H. Hart, S. Nimphius, T. Rantalainen, A. Ireland, A. Siafarikas, R. U. Newton, *J. Musculoskeletal Neuronal Interact.* **2017**, *17*, 114.
[5] B. Clarke, *Clin. J. Am. Soc. Nephrol.* **2008**, *3*, S131.
[6] M. L. Knothe Tate, R. Steck, M. R. Forwood, P. Niederer, *J. Exp. Biol.* **2000**, *203*, 2737.
[7] S. Weinbaum, S. C. Cowin, Y. Zeng, *J. Biomech.* **1994**, *27*, 339.
[8] C. R. Jacobs, C. E. Yellowley, B. R. Davis, Z. Zhou, J. M. Cimbala, H. J. Donahue, *J. Biomech.* **1998**, *31*, 969.
[9] A. G. Robling, C. H. Turner, *Crit. Rev. Eukaryotic Gene Expression* **2009**, *19*, 319.
[10] T. J. Cunningham, M. S. Yu, W. L. McKeithan, S. Spiering, F. Carrette, C.-T. Huang, P. J. Bushway, M. Tierney, S. Albini, M. Giacca, M. Mano, P. L. Puri, A. Sacco, P. Ruiz-Lozano, J.-F. Riou, M. Umbhauer, G. Duester, M. Mercola, A. R. Colas, *Genes Dev.* **2017**, *31*, 1325.
[11] S. W. Cochrane, Y. Zhao, R. S. Welner, X.-H. Sun, *Blood* **2009**, *113*, 1016.
[12] L. S. de la Peña, P. C. Billings, J. L. Fiori, J. Ahn, F. S. Kaplan, E. M. Shore, *J. Bone Miner. Res.* **2005**, *20*, 1168.
[13] N. K. Kanakaris, G. Petsatodis, M. Tagil, P. V Giannoudis, *Injury* **2009**, *40*, S21.
[14] O. P. Gautschi, S. P. Frey, R. Zellweger, *ANZ J. Surg.* **2007**, *77*, 626.
[15] G. B. Bishop, T. A. Einhorn, *Int. Orthop.* **2007**, *31*, 721.
[16] P. Kloen, D. Lauzier, R. C. Hamdy, *Bone* **2012**, *51*, 59.
[17] P. V. Giannoudis, T. A. Einhorn, *Injury* **2009**, *40*, S1.
[18] A. W. James, G. LaChaud, J. Shen, G. Asatrian, V. Nguyen, X. Zhang, K. Ting, C. Soo, *Tissue Eng., Part B* **2016**, *22*, 284.
[19] J. Kopf, A. Petersen, G. N. Duda, P. Knaus, *BMC Biol.* **2012**, *10*, 37.
[20] Y. Zu, X. Liang, J. Du, S. Zhou, C. Yang, *J. Biomech.* **2015**, *48*, 3950.
[21] C. Rauch, A. C. Brunet, J. Deleule, E. Farge, *Am. J. Physiol.: Cell Physiol.* **2002**, *283*, C235.
[22] C. Schwarz, D. Wulsten, A. Ellinghaus, J. Lienau, B. M. Willie, G. N. Duda, *Tissue Eng., Part A* **2013**, *19*, 247.
[23] V. E. E. Galkin, A. Orlova, E. H. H Egelman, *Curr. Biol.* **2012**, *22*, R96.
[24] G. Romet-Lemonne, A. Jégou, *Eur. J. Cell Biol.* **2013**, *92*, 333.
[25] P. Müller, A. Langenbach, A. Kaminski, J. Rychly, J. Planell, *PLoS One* **2013**, *8*, e71283.
[26] H. Sonowal, A. Kumar, J. Bhattacharyya, P. K. Gogoi, B. G. Jaganathan, *J. Biomed. Sci.* **2013**, *20*, 71.
[27] M. Fischer, P. Rikeit, P. Knaus, C. Coirault, *Front. Physiol.* **2016**, *7*, 41.
[28] S. Busche, A. Descot, S. Julien, H. Genth, G. Posern, *J. Cell Sci.* **2008**, *121*, 1025.
[29] G. Posern, R. Treisman, *Trends Cell Biol.* **2006**, *16*, 588.
[30] G. Halder, S. Dupont, S. Piccolo, *Nat. Rev. Mol. Cell Biol.* **2012**, *13*, 591.
[31] B. Zhao, K. Tumaneng, K.-L. Guan, *Nat. Cell Biol.* **2011**, *13*, 877.
[32] S. Dupont, L. Morsut, M. Aragona, E. Enzo, S. Giulitti, M. Cordenonsi, F. Zanconato, J. L. Digabel, M. Forcato, S. Bicciato, N. Elvassore, S. Piccolo, *Nature* **2011**, *474*, 179.
[33] H. Nakajima, K. Yamamoto, S. Agarwala, K. Terai, H. Fukui, S. Fukuhara, K. Ando, T. Miyazaki, Y. Yokota, E. Schmelzer, H.-G. Belting, M. Affolter, V. Lecaudey, N. Mochizuki, *Dev. Cell* **2017**, *40*, 523e6.
[34] B. Zhao, X. Ye, J. Yu, L. Li, W. Li, S. Li, J. Yu, J. D. Lin, C.-Y. Wang, A. M. Chinnaiyan, Z.-C. Lai, K.-L. Guan, *Genes Dev.* **2008**, *22*, 1962.
[35] K. I. Watt, R. Judson, P. Medlow, K. Reid, T. B. Kurth, J. G. Burniston, A. Ratkevicius, C. De Bari, H. Wackerhage, *Biochem. Biophys. Res. Commun.* **2010**, *393*, 619.
[36] J. H. Hong, M. B. Yaffe, *Cell Cycle* **2006**, *5*, 176.
[37] J. Dong, G. Feldmann, J. Huang, S. Wu, N. Zhang, S. A. Comerford, M. F. Gayyed, R. A. Anders, A. Maitra, D. Pan, *Cell* **2007**, *130*, 1120.
[38] H. Zhang, C.-Y. Liu, Z.-Y. Zha, B. Zhao, J. Yao, S. Zhao, Y. Xiong, Q.-Y. Lei, K.-L. Guan, *J. Biol. Chem.* **2009**, *284*, 13355.
[39] B. Zhao, X. Wei, W. Li, R. S. Udan, Q. Yang, J. Kim, J. Xie, T. Ikenoue, J. Yu, L. Li, P. Zheng, K. Ye, A. Chinnaiyan, G. Halder, Z.-C. Lai, K.-L. Guan, *Genes Dev.* **2007**, *21*, 2747.
[40] K.-I. Wada, K. Itoga, T. Okano, S. Yonemura, H. Sasaki, *Development* **2011**, *138*, 3907.

**ADVANCED
SCIENCE NEWS**

www.advancedsciencenews.com

**ADVANCED
BIOLOGY**

www.advanced-bio.com

[41] B. Zhao, Q. Y. Lei, K. L. Guan, *Curr. Opin. Cell Biol.* **2008**, *20*, 638.

[42] S. Strano, E. Munarriz, M. Rossi, L. Castagnoli, Y. Shaul, A. Sacchi, M. Oren, M. Sudol, G. Cesareni, G. Blandino, *J. Biol. Chem.* **2001**, *276*, 15164.

[43] X. Zhi, D. Zhao, Z. Zhou, R. Liu, C. Chen, *Am. J. Pathol.* **2012**, *180*, 2452.

[44] A. Komuro, M. Nagai, N. E. Navin, M. Sudol, *J. Biol. Chem.* **2003**, *278*, 33334.

[45] A. Passaniti, J. L. Brusgard, Y. Qiao, M. Sudol, M. Finch-Edmondson, *Adv. Exp. Med. Biol.* **2017**, *962*, 435.

[46] C. Alarcón, A.-I. Zaromytidou, Q. Xi, S. Gao, J. Yu, S. Fujisawa, A. Barlas, A. N. Miller, K. Manova-Todorova, M. J. Macias, G. Sapkota, D. Pan, J. Massagué, *Cell* **2009**, *139*, 757.

[47] E. Aragon, N. Goerner, A.-I. Zaromytidou, Q. Xi, A. Escobedo, J. Massagué, M. J. Macias, *Genes Dev.* **2011**, *25*, 1275.

[48] X. Varelas, P. Samavarchi-Tehrani, M. Narimatsu, A. Weiss, K. Cockburn, B. G. Larsen, J. Rossant, J. L. Wrana, *Dev. Cell* **2010**, *19*, 831.

[49] K. Grannas, L. Arngården, P. Lönn, M. Mazurkiewicz, A. Blokzijl, A. Zieba, O. Söderberg, *J. Mol. Biol.* **2015**, *427*, 3407.

[50] A. J. Jorgenson, K. M. Choi, D. Sicard, K. M. J. Smith, S. E. Hiemer, X. Varelas, D. J. Tschumperlin, *Am. J. Physiol.: Cell Physiol.* **2017**, *312*, C277.

[51] L. T. Y. Ho, N. Skiba, C. Ullmer, P. V Rao, *Invest. Opthalmol. Visual Sci.* **2018**, *59*, 1969.

[52] J. Ying, P. Wang, S. Zhang, T. Xu, L. Zhang, R. Dong, S. Xu, P. Tong, C. Wu, H. Jin, *Life Sci.* **2018**, *192*, 84.

[53] A. I. Alford, K. M. Kozloff, K. D. Hankenson, *Int. J. Biochem. Cell Biol.* **2015**, *65*, 20.

[54] A. L. Boskey, *Connect. Tissue Res.* **1996**, *35*, 357.

[55] G. E. Sroga, D. Vashishth, *Curr. Osteoporosis Rep.* **2012**, *10*, 141.

[56] A. M. Rodrigues, J. Caetano-Lopes, A. C. Vale, B. Vidal, A. Lopes, I. Aleixo, J. Polido-Pereira, A. Sepriano, I. P. Perpétuo, J. Monteiro, M. F. Vaz, J. E. Fonseca, H. Canhão, *Bone* **2012**, *51*, 981.

[57] S. Tanaka, K. Narusawa, H. Onishi, M. Miura, A. Hijioka, Y. Kanazawa, S. Nishida, S. Ikeda, T. Nakamura, *Osteoporosis Int.* **2011**, *22*, 587.

[58] Y. Tang, R. G. Rowe, E. L. Botvinick, A. Kurup, A. J. Putnam, M. Seiki, V. M. Weaver, E. T. Keller, S. Goldstein, J. Dai, D. Begun, T. Saunders, S. J. Weiss, *Dev. Cell* **2013**, *25*, 402.

[59] J. Kopf, P. Paarmann, C. Hiepen, D. Horbelt, P. Knaus, *BioFactors* **2013**, *40*, 171.

[60] S. Schreivogel, V. Kuchibhotla, P. Knaus, G. N. Duda, A. Petersen, *J. Tissue Eng. Regener. Med.* **2019**, *13*, 1992.

[61] M. L. Knothe Tate, U. Knothe, P. Niederer, *Am. J. Med. Sci.* **1998**, *316*, 189.

[62] S. A. Harris, R. J. Enger, B. L. Riggs, T. C. Spelsberg, *J. Bone Miner. Res.* **1995**, *10*, 178.

[63] A. D. van der Meer, A. A. Poot, J. Feijen, I. Vermes, *Biomicrofluidics* **2010**, *4*, 011103.

[64] D. W. Huang, B. T. Sherman, R. A. Lempicki, *Nat. Protoc.* **2009**, *4*, 44.

[65] J. Yoo, M. Ghiassi, L. Jirmanova, A. G. Balliet, B. Hoffman, A. J. Fornace Jr, D. A. Liebermann, E. P. Bottinger, A. B. Roberts, *J. Biol. Chem.* **2003**, *278*, 43001.

[66] K. Ijiri, L. F. Zerbini, H. Peng, R. G. Correa, B. Lu, N. Walsh, Y. Zhao, N. Taniguchi, X.-L. Huang, H. Otu, H. Wang, J. F. Wang, S. Komiya, P. Ducy, M. U. Rahman, R. A. Flavell, E. M. Gravallese, P. Oettgen, T. A. Libermann, M. B. Goldring, *J. Biol. Chem.* **2005**, *280*, 38544.

[67] F. Ramírez, D. P. Ryan, B. Grüning, V. Bhardwaj, F. Kilpert, A. S. Richter, S. Heyne, F. Dündar, T. Manke, *Nucleic Acids Res.* **2016**, *44*, W160.

[68] E. Afgan, D. Baker, B. Batut, M. van den Beek, D. Bouvier, M. Cech, J. Chilton, D. Clements, N. Coraor, B. A. Grüning, A. Guerler, J. Hillman-Jackson, S. Hiltemann, V. Jalili, H. Rasche, N. Soranzo, J. Goecks, J. Taylor, A. Nekrutenko, D. Blankenberg, *Nucleic Acids Res.* **2018**, *46*, W537.

[69] M. C. Frith, U. Hansen, Z. Weng, *Bioinformatics* **2001**, *17*, 878.

[70] M. Morikawa, D. Koinuma, S. Tsutsumi, E. Vasilaki, Y. Kanki, C.-H. Heldin, H. Aburatani, K. Miyazono, *Nucleic Acids Res.* **2011**, *39*, 8712.

[71] C. Stein, A. F. Bardet, G. Roma, S. Bergling, I. Clay, A. Ruchti, C. Agarinis, T. Schmelzle, T. Bouwmeester, D. Schübeler, A. Bauer, *PLoS Genet.* **2015**, *11*, e1005465.

[72] J. Zhou, P.-L. Lee, C.-I. Lee, S.-Y. Wei, S. H. Lim, T.-E. Lin, S. Chien, J.-J. Chiu, *J. Thromb. Haemostasis* **2013**, *11*, 741.

[73] I. S. Kim, Y. M. Song, T. H. Cho, J. Y. Kim, F. E. Weber, S. J. Hwang, *J. Biomech.* **2009**, *42*, 2721.

[74] G. Chen, C. Deng, Y.-P. Li, *Int. J. Biol. Sci.* **2012**, *8*, 272.

[75] L. Yu, X. Ma, J. Sun, J. Tong, L. Shi, L. Sun, J. Zhang, *Mol. Med. Rep.* **2017**, *16*, 8699.

[76] C. D. Kegelman, D. E. Mason, J. H. Dawahare, G. D. Vigil, S. S. Howard, T. M. Bellido, A. G. Robling, J. D. Boerckel, *bioRxiv* **2017**, 143982.

[77] J. X. Pan, L. Xiong, K. Zhao, P. Zeng, B. Wang, F.-L. Tang, D. Sun, H.-H. Guo, X. Yang, S. Cui, W.-F. Xia, L. Mei, W.-C. Xiong, *Bone Res.* **2018**, *6*, 18.

[78] Q. Zhang, Y. Guo, H. Yu, Y. Tang, Y. Yuan, Y. Jiang, H. Chen, P. Gong, L. Xiang, *J. Cell. Physiol.* **2019**, *234*, 13969.

[79] J. Xiong, M. Almeida, C. A. O'Brien, *Bone* **2018**, *112*, 1.

[80] T. O. Monroe, M. C. Hill, Y. Morikawa, J. P. Leach, T. Heallen, S. Cao, P. H. L. Krijger, W. de Laat, X. H. T. Wehrens, G. G. Rodney, J. F. Martin, *Dev. Cell* **2019**, *48*, 765e7.

[81] M. Kim, T. Kim, R. L. Johnson, D.-S. Lim, *Cell Rep.* **2015**, *11*, 270.

[82] A. Skibinski, J. L. Breindel, A. Prat, P. Galván, E. Smith, A. Rolfs, P. B. Gupta, J. LaBaer, C. Kuperwasser, *Cell Rep.* **2014**, *6*, 1059.

[83] R. E. Hillmer, B. A. Link, *Cells* **2019**, *8*, 502.

[84] N. Sykaras, L. A. Opperman, *J. Oral Sci.* **2003**, *45*, 57.

[85] M. J. Lee, M. R. Byun, M. Furutani-Seiki, J. H. Hong, H. S. Jung, *J. Invest. Dermatol.* **2014**, *134*, 518.

[86] D. Lai, X. Yang, *Cell Signal.* **2013**, *25*, 1720.

[87] R. N. Judson, A. M. Tremblay, P. Knopp, R. B. White, R. Urcia, C. De Bari, P. S. Zammit, F. D. Camargo, H. Wackerhage, *J. Cell Sci.* **2012**, *125*, 6009.

[88] E. Wingender, X. Chen, R. Hehl, H. Karas, I. Liebich, V. Matys, T. Meinhardt, M. Prüss, I. Reuter, F. Schacherer, *Nucleic Acids Res.* **2000**, *28*, 316.

[89] A. Anbanandam, D. C. Albarado, C. T. Nguyen, G. Halder, X. Gao, S. Veeraraghavan, *Proc. Natl. Acad. Sci. USA* **2006**, *103*, 17225.

[90] S. E. Hiemer, A. D. Szymaniak, X. Varelas, *J. Biol. Chem.* **2014**, *289*, 13461.

[91] F. Neto, A. Klaus-Bergmann, Y. T. Ong, S. Alt, A.-C. Vion, A. Szymborska, J. R. Carvalho, I. Hollfinger, E. Bartels-Klein, C. A. Franco, M. Potente, H. Gerhardt, *elife* **2018**, *7*, e31037.

[92] K. Arvidson, B. M. Abdallah, L. A. Applegate, N. Baldini, E. Cenni, E. Gomez-Barrena, D. Granchi, M. Kassem, Y. T. Konttinen, K. Mustafa, D. P. Pioletti, A. Sillat, A. Finne-Wistrand, *J. Cell. Mol. Med.* **2011**, *15*, 718.

[93] A. L. Boskey, R. Coleman, *J. Dent. Res.* **2010**, *89*, 1333.

[94] J. Y. Reginster, N. Burlet, *Bone* **2006**, *38*, 4.

[95] M. D. Robinson, D. J. McCarthy, G. K. Smyth, *Bioinformatics* **2010**, *26*, 139.

[96] T. I. Lee, S. E. Johnstone, R. A. Young, *Nat. Protoc.* **2006**, *1*, 729.

[97] U. K. Laemmli, *Nature* **1970**, *227*, 680.

[98] O. Korchynskyi, P. ten Dijke, *J. Biol. Chem.* **2002**, *277*, 4883.